pISSN 1738-2696 · eISSN 2212-5469
http://dx.doi.org/10.1007/s13770-016-9061-x
ORIGINAL ARTICLE

TERM

Porous Crosslinked Polycaprolactone Hydroxyapatite Networks for Bone Tissue Engineering

Narjes Koupaei[1], Akbar Karkhaneh[2]*

[1]Department of Biomedical Engineering, Science and Research Branch, Islamic Azad University, Tehran, Iran
[2]Department of Biomedical Engineering, Amirkabir University of Technology (Tehran Polytechnic), Tehran, Iran

In this study, porous scaffolds were produced by a thermal crosslinking of polycaprolactone diacrylate in the presence of hydroxyapatite (HA) and particulate leaching technique with sodium chloride as the water soluble porogen for bone tissue engineering applications. The prepared scaffolds were characterized using techniques such as Field Emission Scanning Electron Microscopy, Differential Scanning Calorimetry, and Attenuated Total Reflectance-Fourier Transform Infrared Spectroscopy. Moreover, dynamic mechanical properties were investigated using Dynamic Mechanical Thermal Analysis. The obtained scaffolds present a porous structure with interconnected pores and porosity around 73%. It was found that the incorporation of HA particles to polycaprolactone (PCL) matrix resulted in an increased crystallinity. Moreover, both the storage modulus (E′) and glass transition temperature (T_g) increased, while the loss factor (tan δ) decreased due to the hindrance of the HA particles to the mobility of polymer segments. Cytocompatability of the scaffolds was assessed by MTT assay and cell attachment studies. Osteoconductivity of the scaffolds was investigated with cells alkaline phosphatase extraction. The levels of alkaline phosphatase activity were found to be higher for PCL/HA network scaffold than for PCL network scaffold. In addition, cytocompatibility of the PCL/HA network scaffold indicated no toxicity, and cells were attached and spread to the scaffold walls.

Tissue Eng Regen Med 2016;13(3):251-260

Key Words: Scaffold; Polycaprolactone diacrylate; Hydroxyapatite; Thermal crosslinking

INTRODUCTION

Tissue engineering has attracted enormous attention over the past two decades [1]. Scaffold is one of the key items in tissue engineering and can provide a certain 3D topological guide during tissue regeneration [2]. In tissue engineering and regenerative medicine, several polymers have been used to produce scaffolds to guide the formation of a new tissue [3]. Among them, polycaprolactone (PCL) is one of the most popular Food and Drug Administration approved polymers [4]. PCL is often used as a biodegradable and noncytotoxic biomaterial for the production of scaffolds for tissue engineering [5,6]. Recently, a series of crosslinkable polymers such as polycaprolactone diacrylate (PCLDA), poly propylene fumarate, and poly caprolactone fumarate (PCLF) have gained attraction for tissue engineering applications [7,8]. Among them, PCLDA is a good candidate for hard tissue engineering applications. The major shortcoming associated with the application of PCLDA in bone tissue engineering is its lack of bioactive functional result in a poor cell adhesion, which is a critical issue for successful *in vitro* cell culture and subsequent tissue formation [9,10]. Kweon et al. [11] developed a biodegradable scaffold made of crosslinkable PCLDA. They reported that PCL network is not sufficient for bone marrow conductance and needs additional conducting materials for cell attachment and supporting cell proliferation. Moreover, they showed that the compressive modulus of porous crosslinked PCLDA was higher than that of PCL due to the crosslinking between PCL molecules [11]. Both the conventional PCL and PCLDA exhibit small cell adhesion. On the other hand, hydroxyapatite (HA) is a ceramic material with a composition and structure close to natural bone mineral and is biocompatible, osteoconductive and osteoinductive [12]. Despite its inherent osteoconductivity, HA has some undesirable traits, such as brittleness and difficulty of shaping. As a result, the fabrication of a biodegradable polymer in combination with the bioceramic could be a solution to such problems [7,13]. Chuenjitkuntaworn et al. [13] have shown that electrospun PCL/HA fibrous matrices could support much better cell attachment, pro-

Received: July 17, 2015
Revised: September 1, 2015
Accepted: September 8, 2015
***Corresponding author:** Akbar Karkhaneh, Department of Biomedical Engineering, Amirkabir University of Technology (Tehran Polytechnic), Tehran 15875-4413, Iran.
Tel: 98-2164542496, E-mail: a.karkhaneh@aut.ac.ir

liferation, differentiation, and *in vitro* mineralization of human osteosarcoma cells than did the PCL, indicating that PCL/HA could be a suitable material for bone scaffolding. HA has been incorporated with numerous polymer matrices to improve their mechanical properties, protein absorption and osteoconductivity [12,14,15].

Researchers have combined PCL with HA particles to produce composite scaffolds for bone regeneration, but in this work we used crosslinkable polymer (PCLDA). This study focused on rendering PCL into crosslinkable biomaterial and also improved the bioactivity and mechanical properties of PCL through incorporating HA particles with PCL, crosslinking reaction, and network formation. The microstructure and characteristics of the PCL and PCL/HA networks scaffold were investigated. In addition, to evaluate the cell-scaffold interaction, MG-63 cells were cultured in the scaffolds for 6 and 24 hours, and the morphology of cell attachment was observed by scanning electron microscopy.

MATERIALS AND METHODS

Materials

Polycaprolactone diol (PCL diol, M_n=2000) and 2,2-Azobisisobutyronitrile (AIBN) were obtained from Sigma-Aldrich. Benzene, n-hexane, acryloyl chloride, triethylamine (TEA), and HA powder with sizes in the range of 0.1−40 μm were purchased from Merck. 1, 4-Dioxane was from AppliChem. The porogen is sodium chloride (NaCl) powder with sizes in the range of 105−250 μm.

Synthesis of PCL diacrylate

PCLDA was synthesized by reacting PCL diol with acryloyl chloride in the presence of TEA as the proton scavenger [16]. Briefly, 5 g of PCL diol was dissolved in 40 mL of benzene. 0.866 mL of TEA and 0.505 mL of acryloyl chloride were added to the solution, and the mixture was stirred for 3 h at 80°C. The reaction mixture was filtered to remove TEA hydrochloride and precipitated into excess n-hexane to obtain PCLDA; afterwards, it was dried under vacuum for 24 h.

Preparation of PCL/HA networks scaffold

PCL/HA scaffolds were prepared by thermal-crosslinking particulate-leaching technique. 30% (w/v) of PCLDA dissolved in dioxane. 5 wt.% of HA, a small amount of AIBN and 140% (w/v) of NaCl particulates as porogen were mixed with PCLDA solution. Homogeneous PCLDA/AIBN/HA/NaCl mixture was transferred into test tube and was placed in an oven at 70°C for 12 h. The resulting crosslinked samples were removed from the tube and were cut into discs. Afterwards, the NaCl particulates were leached out by immersing the samples in distilled water for 4 days at room temperature in a shaking plate, in order to completely remove the porogen. Finally, the scaffolds were freeze-dried for 2 days.

Characterization

Fourier transform infrared spectroscopy and ^{1}H nuclear magnetic resonance

The synthesized PCLDA were characterized by Fourier transform infrared spectroscopy (FTIR, Jasco, Tokyo, Japan) and ^{1}H nuclear magnetic resonance (^{1}H-NMR, Bruker Biospin, Rheinstetteh, Germany) measurements to confirm the formation of PCLDA. Moreover, attenuated total reflectance-Fourier transform infrared spectroscopy (ATR-FTIR, Jasco, Tokyo, Japan) was recorded to analyze the chemical structure of the crosslinked PCLDA and PCLDA/HA specimens.

Differential scanning calorimetry

Differential scanning calorimetry (DSC) was performed in a Pyris 6 apparatus (Perkin-Elmer, CT, USA) under nitrogen atmosphere. To keep the same thermal history, samples were first heated from room temperature to 100°C and cooled to 0°C at a cooling rate of 10°C/min. Then a subsequent heating run was performed from 0°C to 100°C at a rate of 10°C/min.

Electron microscopy studies

The cross-section morphology of the scaffolds was examined using field emission scanning electron microscopy (FESEM, Zeiss, Oberkocken, Germany). The scaffolds were fractured in liquid nitrogen and were coated with gold. The average pore size of the scaffolds was evaluated from geometrical measurements of randomly selected 20 pores on the scanning electron micrographs.

Measurement of porosity

The porosity of the scaffold was determined using a density bottle based on Archimedes' Principle according to a known technique [17-19]. Ethanol was used as the displacement liquid. In brief, the porosity of scaffold was calculated by the following equation (1):

$$\text{Porosity (\%)} = \frac{(W_2 - W_3 - W_S)/\rho_e}{(W_1 - W_3)/\rho_e} \times 100 \quad \text{Equation (1)}$$

where W_1 is the weight of density bottle filled with ethanol, W_2 is the weight of density bottle including ethanol and scaffold, W_3 is the weight of density bottle taken out ethanol-saturated scaffold from W_2, W_S is the weight of scaffold, ρ_e is the density of ethanol, $(W_1-W_3)/\rho_e$ is the total volume of the scaffold including pores, and $(W_2-W_3-W_S)/\rho_e$ is the pore volume in the scaffold.

Dynamic mechanical thermal analysis

The dynamic mechanical behavior of the crosslinked PCLDA and PCLDA/HA networks was studied by DMTA using a UK Polymer Lab model MK-II analyzer in compression mode. The range of temperature was from -80 to 100°C at a heating rate of 5°C min^{-1}. The measurements were performed at a frequency of 1 Hz. The storage modulus (E') and loss factor (tan δ) were recorded as a function of temperature. Glass temperature (T_g) was taken of the maximum of loss factor curve.

Cell studies

The biological properties of the scaffolds were evaluated with osteosarcoma cell line MG63 (National Cell Bank of Iran, Pasteur Institute of Iran). Briefly, cells were cultured in Dulbecco's Modified Eagle's Medium (DMEM, GIBCO, Paisley, UK)/supplemented with 10% (v/v) fetal bovine serum (FBS, Seromed, Berlin, Germany), 100 U mL^{-1} penicillin and 100 μg mL^{-1} streptomycin. Cells were incubated at 37°C in a humidified atmosphere of 5% CO_2 and 95% air. Cultured cells were trypsinized, suspended in fresh culture medium and seeded on each scaffold at a concentration of 1×10^4 cells. Prior to cell seeding, scaffolds were sterilized using UV treatment.

MTT assay

The cell viability performance of 3 and 7 days extracted scaffolds was evaluated using the MTT assay method. MTT assay was done in indirect contact testing. For the assay, cells were placed into a 96 well plate at a density of 1×10^4 cells/well and were incubated under standard culturing conditions. At the end of the incubation period, the media were replaced by the extract and incubated for another 24 h, and then 100 μL of 0.5 mg mL^{-1} MTT solution was added into each well. After that, the plate was incubated at 37°C for 4 h. Then, the medium was removed, 100 μL of isopropanol solution was added and further incubated for 15 min in order to enhance the dissolution of the formazan crystal. The optical density (OD) of formazan in the solution was detected by a multiwall microplate reader (STAT FAX 2100, Pam City, USA) at 545 nm. For the reference purpose, cells were seeded into a fresh culture medium (control) with the same seeding conditions. Results were expressed by means of measurements (n=4) with error bars representing the standard deviation.

Alkaline phosphatase activity

The alkaline phosphatase activity (ALP) was assayed by the hydrolysis of p-nitrophenol phosphate as the release of p-nitrophenol from p-nitrophenol phosphate [20-22]. ALP activity was done in direct contact testing. The cells were cultured at a density of 1×10^4 cells on each scaffold in 24-well culture plates. After 7 and 14 days, the amount of ALP released by cells to the medium in each well was determined by Autoanalyzer (Hitachi 717, Tokyo, Japan) using Pars Azmon kit (Pars Azmoon Inc., Tehran, Iran). The enzyme activity was expressed as unit/letre. The culture medium with the same amount of cells was considered as control.

Cell morphology

Morphological characteristics of cells on the surface of scaffolds were investigated 6 and 24 hours after seeding using scanning electron microscope (SEM, KYKY-EM-3200). Cells grown on the scaffolds were first washed with PBS, fixed with 4% glutaraldehyde and dehydrated in graded series of ethanol and dried in vacuum overnight. The dry scaffolds were coated with gold and were observed by SEM.

Statistical analysis

Statistical comparisons were performed using one-way analysis of variance ANOVA with the "Turkey's Post Hoc test". *p* values<0.05 were considered statistically significant.

RESULTS

Preparation of PCL/HA networks scaffold

As a crosslinkable biodegradable polymer, PCLDA was synthesized by the reaction of PCL diol with acryloyl chloride. The chemical structure of PCLDA was confirmed by FTIR and ^{1}H-NMR measurements. From the FTIR spectra of PCL diol and PCLDA, PCLDA showed absorption bands at 813 and 1635 cm^{-1} assigned to the C=C due to the acrylation of PCL diol. The peaks were not observed in PCL diol itself. PCLDA demonstrated vinyl groups at the range of 5.79−6.43 ppm could be confirmed from the corresponding ^{1}H-NMR spectrum [16]. From the above results, the terminal hydroxyl groups in the PCL diol were converted to acrylate groups by the reaction with acryloyl chloride (data not shown).

Biodegradable crosslinked PCLDA and PCLDA/HA networks, were prepared by thermal polymerization of the PCLDA. The ATR-FTIR spectra of crosslinked PCLDA and PCLDA/HA are shown in Figure 1. The absorption peaks at 1725 and 2950 cm^{-1} were assigned to ester carbonyl and methylene groups, respectively. The peaks for vinyl groups at 813 and 1635 cm-1 observed in the spectrum of PCLDA were not evident for the crosslinked networks, indicating complete consumption of unsaturated double bonds in crosslinking. The absorption peak for phosphate (PO_4) group of HA at around 1029 cm^{-1} [15] was observed in the spectrum of crosslinked PCLDA/HA.

SEM analysis

Porous scaffolds were fabricated by a thermal crosslinking par-

ticulate leaching technique with NaCl as the water soluble porogen. Scanning electron microscope can qualitatively evaluate morphology and pore size. The cross-sections of NaCl-leached scaffolds are shown in the SEM images presented in Figure 2.

Due to the random porogen distribution in the bulk, the resulting scaffolds exhibited irregular pore structures as shown in Figure 2. Both scaffolds are highly porous, a structure favorable for cell attachment and new bone tissue ingrowth [23]. Pore interconnectivity plays an important role in promoting the ingrowth of cells and new tissue. Good interconnectivity is believed to be beneficial to the flow transport of nutrients and wastes [24]. The pore interconnectivity can be tailored by the variation in both the size and the content of the porogen particles used and should be studied in our further studies.

The average pore size and porosity of the scaffolds are presented in Table 1. It can be seen that there are no significant differences in the porosity and average pore size for PCL and PCL/HA networks scaffold. Both scaffolds had rather high porosities (over 73%), considered to be beneficial to cell growth and survival.

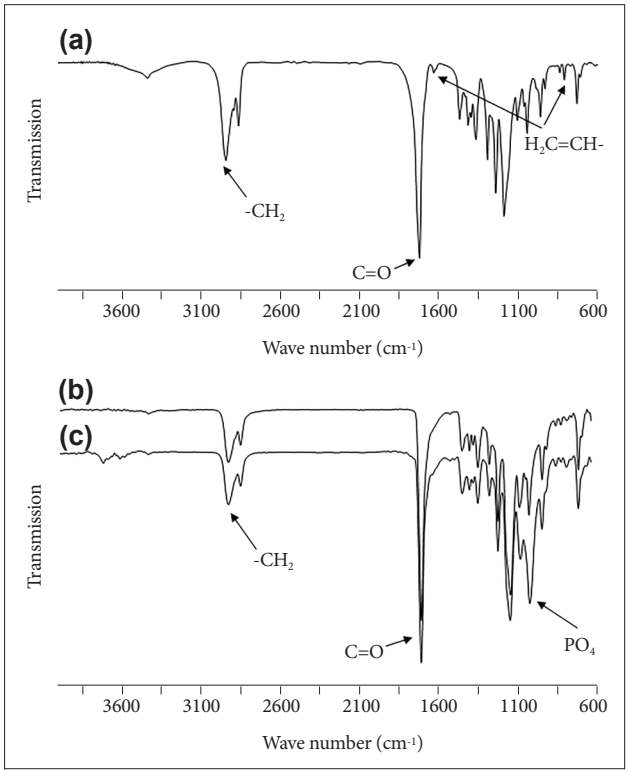

Figure 1. (a) FTIR spectra of PCLDA, (b) ATR-FTIR spectra of Crosslinked PCLDA, and (c) Crosslinked PCLDA/HA. FTIR: fourier transform infrared spectroscopy, PCLDA: polycaprolactone diacrylate, ATR-FTIR: attenuated total reflectance-Fourier transform infrared spectroscopy, HA: hydroxyapatite.

DSC analysis

DSC curves in Figure 3 from the heating run were used to obtain the thermal properties of PCLDA, crosslinked PCLDA and PCLDA/HA networks. The melting temperature (T_m), heat of fusion (ΔH_m), and crystallinity (X_c) are listed in Table 2. The X_c for PCL moiety in the crosslinked networks was calculated using equation (1):

$$X_c\% = [\Delta H_m / (w_{PCL}\, \Delta H_m^c)] \times 100 \quad \text{Equation (1)}$$

where, ΔH_m is the melting enthalpy associated to the PCL peak in the DSC thermograms, ΔH_m^c represents the melting enthalpy of the completely crystalline PCL (135.55 J/g) [25] and w_{PCL} is the weight fraction of PCL in crosslinked networks. Like PCLDA, crosslinked PCLDA and PCLDA/HA networks were semicrystalline with varied T_m and crystallinity. The results showed that the area of the melting peak of PCL was lower in the networks than in pure PCLDA. This indicated that the crystallinity of PCL decreased after crosslinking. After thermal-crosslinking reaction, the mobility of molecular chain was suppressed, resulting in a decrease of PCL crystal formation. Moreover, PCLDA showed a sharp and strong melting peak at 37°C, but the crosslinked PCLDA showed a lower melting peak at 33.5°C. This is because the crosslinks lower the activity of the crystallizable units in the melt, and thus lower the melting temperature [26]. It can be observed from Table 2 that the cystallinity (X_c) increased when PCLDA were crosslinked in the presence of HA particles, which indicated that HA had a nucleating effect on the crystallization of PCL. This behavior is in agreement with the results obtained by Cai et al. [14]. In the polymeric networks, crystallites play a critical role in influencing their mechanical properties. PCL crystallites could enhance the polymer network's mechanical properties, which is important for bone tissue engineering application [8,27].

DMTA analysis

The DMTA results for crosslinked PCLDA and PCLDA/HA are shown in Figure 4. Both networks showed two distinct thermal transitions: the glass transitions (T_g) were evident at -26.3°C and -22.1°C where the initiation of polymer chain mobility occurred, while the melting transitions (T_m) appeared at 39.8°C and 36.7°C. This result is in agreement with those reported by Rodriguez et al. [28] and Averous et al. [29]. As can be seen from Figure 4A, incorporation of HA into the PCLDA resulted in an increased storage modulus over the entire temperature range (-80 to 100°C), indicating that HA has a reinforcing effect on this polyester. The storage modulus reveals the capability of a material to store mechanical energy and resist deformation [30]. Results indicated that the incorporation of HA enhanced the rigidity of the network. Moreover, in our previous study, the com-

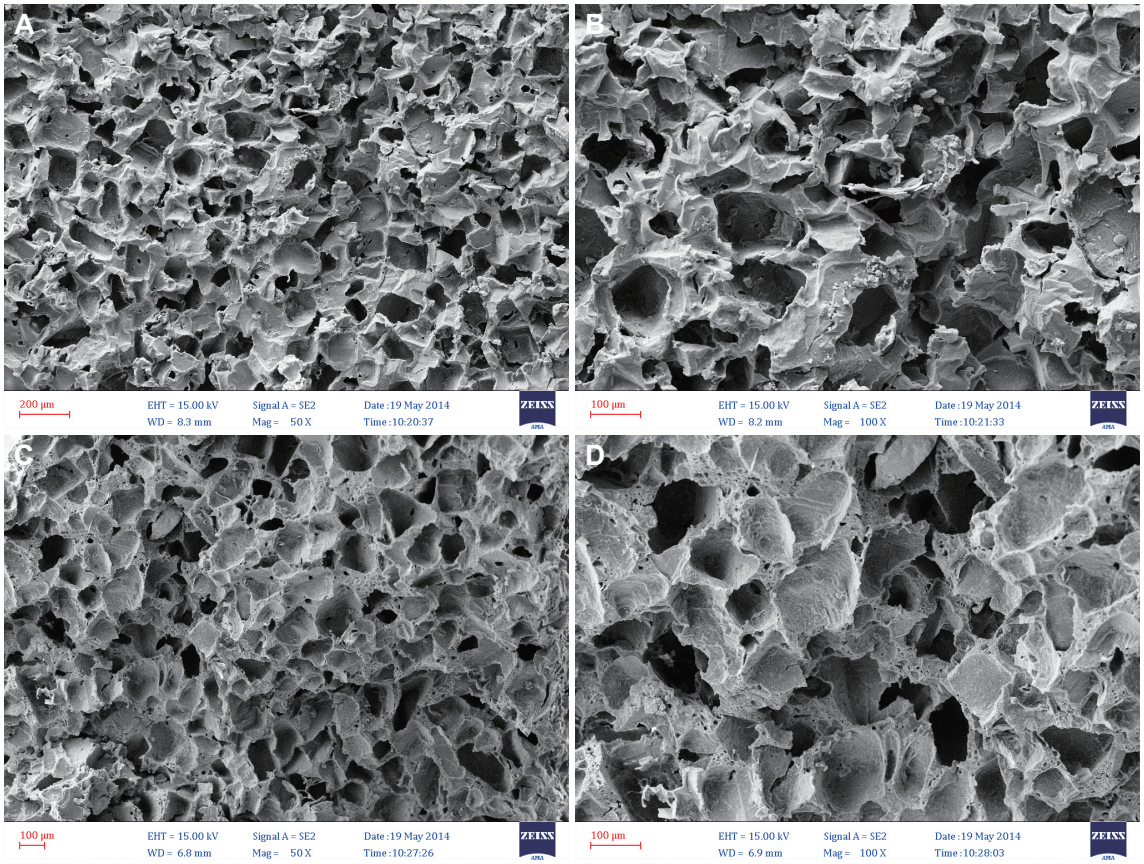

Figure 2. FESEM images of the cross-sectional morphology. (A and B) PCL network scaffolds and (C and D) PCL/HA network scaffolds. FESEM: field emission scanning electron microscopy, PCL: polycaprolactone, HA: hydroxyapatite.

Table 1. Physical property of the PCL and PCL/HA networks scaffold

Physical property	Scaffold samples	
	PCL network	PCL/HA network
Average pore size (μm)	115±32	121±30
Porosity (%)	73.15±1.90	74.11±1

PCL: polycaprolactone, HA: hydroxyapatite

pression stress-strain curves of crosslinked PCL and PCL/HA scaffolds have carried out by a universal testing machine. Results demonstrated the crosslinked PCL/HA scaffold had much better compressive modulus than the crosslinked PCL scaffold, indicating that HA improved mechanical properties of crosslinked PCL scaffold [31]. The values of the storage modulus at 37°C are important if one pretends to use such systems in biomedical applications. The storage modulus of crosslinked PCLDA/HA at 37°C was 30 MPa, significantly higher than 22 MPa for crosslinked PCLDA. As can also be seen from Figure 4B, the glass transition temperature (T_g) determined from the peak of tan δ curve, shifted to a higher temperature accompanied by the addition of HA particles. The HA particles immobilized PCL molecular chains and, hence, increased T_g of the polymer matrix. A similar effect was also observed by other authors when HA was added to PDLLA [32]. The modulus was dropped signifi-

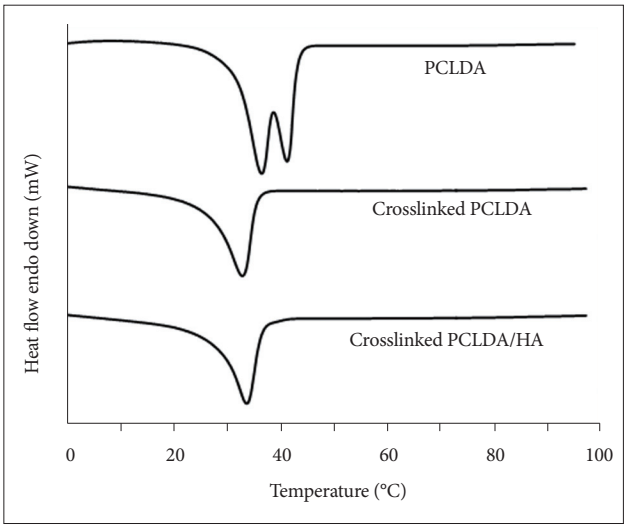

Figure 3. DSC curves of PCLDA, crosslinked PCLDA and PCLDA/HA networks. DSC: differential scanning calorimetry, PCLDA: polycaprolactone diacrylate, HA: hydroxyapatite.

cantly at T_g where segmental chain motions started [33]. Additionally, the tan δ peak of the crosslinked PCLDA/HA network dropped clearly, and a certain broadening of the peak was observed. The variation of the tan δ peak as well as T_g is attributed to the reinforcing effects of homogeneously dispersed HA, which leads to a reduction in mobility of the polymer chains in the amorphous phase [30].

Cell studies

Figure 5 showed the absorbance illustrating of the viability of MG63 cells that were cultured with the 3 and 7 days extracted medium from PCL and PCL/HA networks scaffold. The results showed that there was no significant difference in the OD values in cells treated with both extracts in comparison to the control.

The ALP activity of cultured MG63 cells on PCL and PCL/HA networks scaffold at days 7 and 14 of cell culture has been shown in Figure 6. Our results showed that ALP activity, which is conventionally used as the initial marker for osteoblast activity, was significantly higher for the PCL/HA network scaffold compared to the PCL network scaffold after 14 days of cell culture.

SEM was used to study the attachment and spreading of cells to the scaffolds. More round cells were seen on the PCL/HA network scaffold than on the PCL network scaffold after 6 hours of culture (Fig. 7). After 24 hours of culture, it also revealed that the cells spread on the surface of PCL/HA network scaffold (Fig. 8). These results suggest that cells could attach and spread well on the PCL/HA network scaffold.

Table 2. Thermal properties of PCLDA, crosslinked PCLDA and PCLDA/HA networks

	T_m (°C)	ΔH_m (J/g)	X_C (%)
PCLDA	37	68.2	50.3
Crosslinked PCLDA	33.5	44.9	33.2
Crosslinked PCLDA/HA	34.3	40.5	34.8

PCLDA: polycaprolactone diacrylate, HA: hydroxyapatite

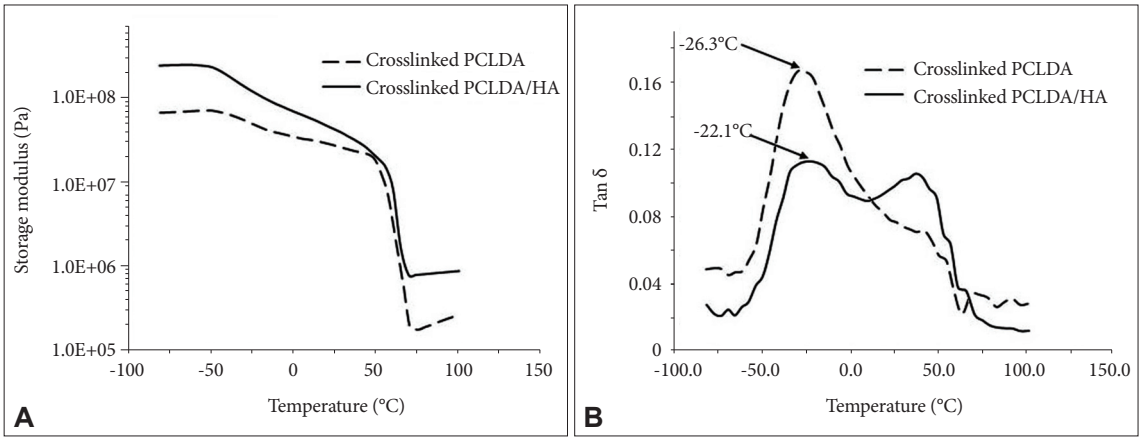

Figure 4. Dynamic thermal mechanical properties of the crosslinked PCLDA and PCLDA/HA. (A) Storage modulus vs. temperature and (B) Tan δ vs. temperature. PCLDA: polycaprolactone diacrylate, HA: hydroxyapatite.

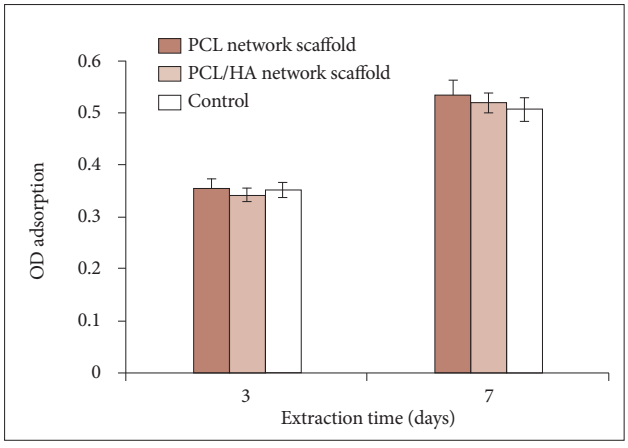

Figure 5. MTT assay showing biocompatibility of the PCL and PCL/HA networks scaffold. MTT: methylthiazol tetrazolium, PCL: polycaprolactone, HA: hydroxyapatite.

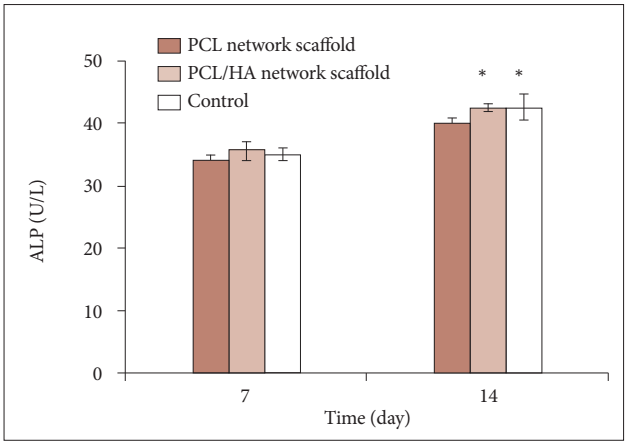

Figure 6. Histogram showing alkaline phosphatase activity of cells after 7 and 14 days of incubation. *p<0.05 compared to the PCL network scaffold. PCL: polycaprolactone.

DISCUSSION

Crosslinking is an effective method of generation of biodegradable scaffolds for tissue-engineering applications. In the present study, the porous scaffolds were fabricated by a thermal crosslinking particulate leaching technique with NaCl as the water soluble porogen. The ATR-FTIR spectra of crosslinked networks were indicated complete consumption of unsaturated double bonds in crosslinking.

SEM was used to evaluate morphology and pore size. Due to the random porogen distribution in the bulk, the resulting scaffolds exhibited irregular pore structures as shown in Figure 2. Both scaffolds are highly porous, a structure favorable for cell attachment and new bone tissue ingrowth [26]. Pore interconnectivity plays an important role in promoting the ingrowth of cells and new tissue. Good interconnectivity is believed to be benefi-

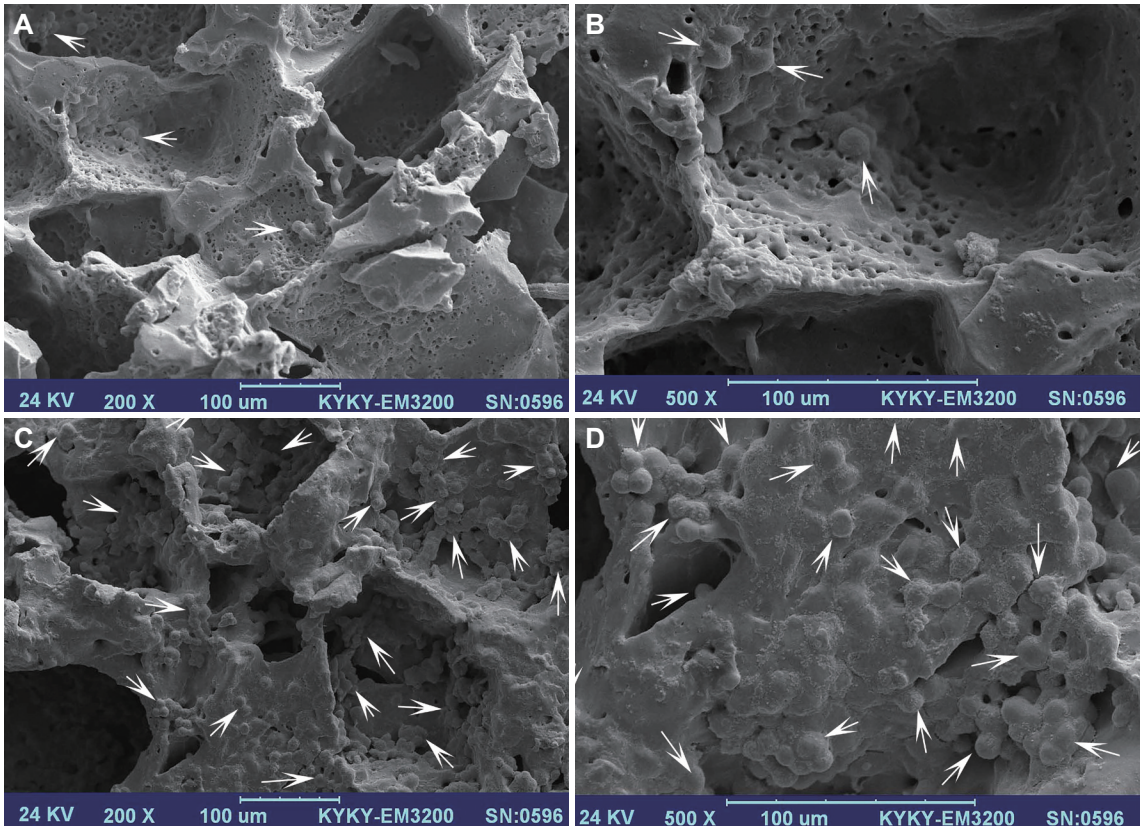

Figure 7. (A and B) SEM images of MG63 cells attached to the surface of the PCL network scaffold, (C and D) PCL/HA network scaffold after 6 h culture. The arrows point to cells. SEM: scanning electron microscopy, PCL: polycaprolactone, HA: hydroxyapatite.

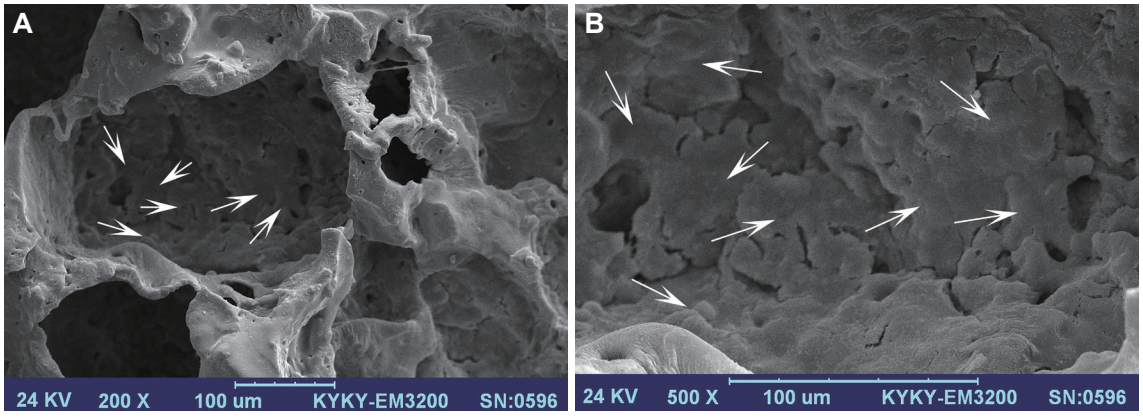

Figure 8. (A) SEM images of MG63 cells spread on the surface of the PCL/HA network scaffold after 24 h culture, (B) is a magnified image of (A). The arrows point to cells. SEM: scanning electron microscopy, PCL: polycaprolactone, HA: hydroxyapatite.

cial to the flow transport of nutrients and wastes [27]. The pore interconnectivity can be tailored by the variation in both the size and the content of the porogen particles used and should be studied in our further studies.

DSC analysis showed that the area of the melting peak of PCL was lower in the networks than in pure PCLDA. This indicated that the crystallinity of PCL decreased after crosslinking. After thermal-crosslinking reaction, the mobility of molecular chain was suppressed, resulting in a decrease of PCL crystal formation. Moreover, PCLDA showed a sharp and strong melting peak at 37°C, but the crosslinked PCLDA showed a lower melting peak at 33.5°C. This is because the crosslinks lower the activity of the crystallizable units in the melt, and thus lower the melting temperature [28]. It can be observed from Table 2 that the cystallinity (X_c) increased when PCLDA were crosslinked in the presence of HA particles, which indicated that HA had a nucleating effect on the crystallization of PCL. This behavior is in agreement with the results obtained by Cai et al. [14]. In the polymeric networks, crystallites play a critical role in influencing their mechanical properties. PCL crystallites could enhance the polymer network's mechanical properties, which is important for bone tissue engineering application [8,29].

It becomes evident from the DMTA test results that incorporation of HA into the PCLDA resulted in an increased storage modulus over the entire temperature range (-80 to 100°C), indicating that HA has a reinforcing effect on this polyester. The storage modulus reveals the capability of a material to store mechanical energy and resist deformation [30]. Results indicated that the incorporation of HA enhanced the rigidity of the network. Moreover, in our previous study, the compression stress-strain curves of crosslinked PCL and PCL/HA scaffolds have carried out by a universal testing machine. Results demonstrated the crosslinked PCL/HA scaffold had much better compressive modulus than the crosslinked PCL scaffold, indicating that HA improved mechanical properties of crosslinked PCL scaffold [31]. The values of the storage modulus at 37°C are important if one pretends to use such systems in biomedical applications. The storage modulus of crosslinked PCLDA/HA at 37°C was 30 MPa, significantly higher than 22 MPa for crosslinked PCLDA. Additionally, the HA particles immobilized PCL molecular chains and, hence, increased T_g of the polymer matrix. A similar effect was also observed by other authors when HA was added to PDLLA [32]. The modulus was dropped significantly at T_g where segmental chain motions started [33]. The variation of the tan δ peak as well as T_g is attributed to the reinforcing effects of homogeneously dispersed hydroxyapatite, which leads to a reduction in mobility of the polymer chains in the amorphous phase [30].

An ideal scaffold should not release toxic products or produce adverse reactions [31]. The MTT analysis was indicated that the developed scaffolds are cytocompatible, and contain no toxic leachable. To investigate the osteocoductivity of the scaffolds, the extraction of ALP enzyme was measured as an indicator of osteoblast activity. A higher level of ALP activity measured for PCL/HA network scaffold possibly suggested that this type of scaffold had a beneficial effect on the growth and phenotype of MG63 cells. In our case, the possible mechanism to promote the activity of osteoblasts might be ascribed to the increased affinity of osteoblasts to the scaffolds and the improved osteoconductive property of scaffolds because of the incorporation of HA particles. It is however, generally accepted that ALP activity would increase in the presence of Ca^{2+} ions, which is reflected in improved osteoblast activity [20]. Moreover, it was found that the ALP activity of MG63 cells on the PCL/HA network scaffold was the same as that on the control for day 14. It seems that the addition of HA particles did not significantly change the roughness of the scaffold surface, which might help the anchorage and attachment of the cells to the surface [34]. Farokhi et al. [7] developed a composite scaffold for bone tissue engineering by combining crosslinkable PCLF with nanohydroxyapatite (nHA). They reported that the values of ALP for PCLF/HA were similar to control, establishing that PCLF/nHA scaffold did not have any harmful effects on ALP production.

Adhesion of cells to biomaterials is a major factor of their biocompatibility and it is postulated that the more compatible the surface, the greater the amount of cell attaching [7]. Moreover, cell attachment is a critical step in initiating cell growth and neotissue development [35]. As shown in Figure 7, more cells were seen on the PCL/HA network scaffold than on the PCL network scaffold after 6 hours of culture. The better cell adhesion on the PCL/HA network scaffold for MG63 cells should be due to the presence of HA, a known osteoconductive material [13]. In addition, the presence of calcium ions in HA particles form sites of positive charges, which aid the adsorption of serum proteins that could help increase the adhesion of the cells [20].

In conclusion, the PCL/HA scaffolds with well interconnected pore structure were fabricated by a thermal crosslinking particulate leaching technique. DMTA analysis showed that T_g-PCL was increased by adding HA particles. Moreover, the reinforcing effect of HA particles on the networks was confirmed by using the dynamic mechanical analysis, from which an increase in the storage modulus was detected due to the addition of HA particles. Initially rounded morphology of MG63 cells is seen during attachment followed by flattened well spread morphology of the cells on the PCL/HA networks scaffold. The scaffolds were also found to be cytocompatible in MTT assay. In addition, a higher level of ALP activity was measured for PCL/HA networks scaffold. Therefore, we concluded that the PCL/HA network scaf-

folds are potential scaffolds for tissue engineering applications.

In conclusion, the PCL/HA scaffolds with well interconnected pore structure were fabricated by a thermal crosslinking particulate leaching technique. DMTA analysis showed that T_g-PCL was increased by adding HA particles. Moreover, the reinforcing effect of HA particles on the networks was confirmed by using the dynamic mechanical analysis, from which an increase in the storage modulus was detected due to the addition of HA particles. Initially rounded morphology of MG63 cells is seen during attachment followed by flattened well spread morphology of the cells on the PCL/HA networks scaffold. The scaffolds were also found to be cytocompatible in MTT assay. In addition, a higher level of ALP activity was measured for PCL/HA networks scaffold. Therefore, we concluded that the PCL/HA network scaffolds are potential scaffolds for tissue engineering applications.

Conflicts of Interest

The authors have no financial conflicts of interest.

Ethical Statement

There are no animal experiments carried out for this article.

REFERENCES

1. Soheilmoghaddam M, SharifzadehGh, HeidarPour R, Wahit MU, Whye WT, Lee XY. Regenerated cellulose/β-cyclodextrin scaffold prepared using ionic liquid. Mater Lett 2014;135:210-213.
2. Lee SH, Lee JH, Cho YS. Analysis of degradation rate for dimensionless surface area of well-interconnected PCL scaffold via in-vitro accelerated degradation experiment. Tissue Eng Regen Med 2014;11:446-452.
3. Lee SH, Chung HY, Shin HI, Park DJ, Choi JH. Osteogenic activity of chitosan-based hybrid scaffold prepared by polyelectrolyte complex formation with alginate. Tissue Eng Regen Med 2014;11:106-112.
4. García Cruz DM, Coutinho DF, Mano JF, Gómez Ribelles JL, Salmerón Sánchez M. Physical interactions in macroporous scaffolds based on poly(ε-caprolactone)/chitosan semi-interpenetrating polymer networks. Polymer 2009;50:2058-2064.
5. Rezaei A, Mohammadi MR. Development of hydroxyapatite nanorods-polycaprolactone composites and scaffolds derived from a novel in-situ sol-gel process. Tissue Eng Regen Med 2012;9:295-303.
6. Park SA, Lee SH, Kim WD. Fabrication of porous polycaprolactone/hydroxyapatite (PCL/HA) blend scaffolds using a 3D plotting system for bone tissue engineering. Bioprocess Biosyst Eng 2011;34:505-513.
7. Farokhi M, Sharifi S, Shafieyan Y, Bagher Z, Mottaghitalab F, Hatampoor A, et al. Porous crosslinked poly(ε-caprolactone fumarate)/nano-hydroxyapatite composites for bone tissue engineering. J Biomed Mater Res A 2012;100:1051-1060.
8. Cai L, Wang S. Poly(ε-caprolactone) acrylates synthesized using a facile method for fabricating networks to achieve controllable physicochemical properties and tunable cell responses. Polymer 2010;51:164-177.
9. Zhang Y, Zhang Y, Chen M, Yan J, Ye Z, Zhou Y, et al. Surface properties of amino-functionalized poly(ε-caprolactone) membranes and the improvement of human mesenchymal stem cell behavior. J Colloid Interface Sci 2012;368:64-69.
10. Chen M, Le DQ, Baatrup A, Nygaard JV, Hein S, Bjerre L, et al. Self-assembled composite matrix in a hierarchical 3-D scaffold for bone tissue engineering. Acta Biomater 2011;7:2244-2255.
11. Kweon H, Yoo MK, Park IK, Kim TH, Lee HC, Lee HS, et al. A novel degradable polycaprolactone networks for tissue engineering. Biomaterials 2003;24:801-808.
12. Wang Y, Liu L, Guo S. Characterization of biodegradable and cytocompatible nano-hydroxyapatite/polycaprolactone porous scaffolds in degradation in vitro. Polym Degrad Stabil 2010;95:207-213.
13. Chuenjitkuntaworn B, Inrung W, Damrongsri D, Mekaapiruk K, Supaphol P, Pavasant P. Polycaprolactone/hydroxyapatite composite scaffolds: preparation, characterization, and in vitro and in vivo biological responses of human primary bone cells. J Biomed Mater Res A 2010;94:241-251.
14. Cai L, Guinn AS, Wang S. Exposed hydroxyapatite particles on the surface of photo-crosslinked nanocomposites for promoting MC3T3 cell proliferation and differentiation. Acta Biomater 2011;7:2185-2199.
15. Jiang CP, Chen YY, Hsieh MF. Biofabrication and in vitro study of hydroxyapatite/mPEG-PCL-mPEG scaffolds for bone tissue engineering using air pressure-aided deposition technology. Mater Sci Eng C Mater Biol Appl 2013;33:680-690.
16. Park JS, Woo DG, Sun BK, Chung HM, Im SJ, Choi YM, et al. In vitro and in vivo test of PEG/PCL-based hydrogel scaffold for cell delivery application. J Control Release 2007;124:51-59.
17. Yang J, Shi G, Bei J, Wang S, Cao Y, Shang Q, et al. Fabrication and surface modification of macroporous poly(L-lactic acid) and poly(L-lactic-co-glycolic acid) (70/30) cell scaffolds for human skin fibroblast cell culture. J Biomed Mater Res 2002;62:438-446.
18. Wu H, Wan Y, Dalai S, Zhang R. Response of rat osteoblasts to polycaprolactone/chitosan blend porous scaffolds. J Biomed Mater Res A 2010;92:238-245.
19. Wan Y, Wu H, Cao X, Dalai S. Compressive mechanical properties and biodegradability of porous poly(caprolactone)/chitosan scaffolds. Polym Degrad Stabil 2008;93:1736-1741.
20. Tahmasbi Rad A, Solati-Hashjin M, Abu Osman NA, Faghihi S. Improved bio-physical performance of hydroxyapatite coatings obtained by electrophoretic deposition at dynamic voltage. Ceram Int 2014;40:12681-12691.
21. Shor L, Güçeri S, Wen X, Gandhi M, Sun W. Fabrication of three-dimensional polycaprolactone/hydroxyapatite tissue scaffolds and osteoblast-scaffold interactions in vitro. Biomaterials 2007;28:5291-5297.
22. Ozkan S, Kalyon DM, Yu X, McKelvey CA, Lowinger M. Multifunctional protein-encapsulated polycaprolactone scaffolds: fabrication and in vitro assessment for tissue engineering. Biomaterials 2009;30:4336-4347.
23. Lee WF, Cheng TS. Studies on preparation and properties of porous biodegradable poly(NIPAAm) hydrogels. J Appl Polym Sci 2008;109:1982-1992.
24. Rodriguez ED, Luo X, Mather PT. Linear/network poly(ε-caprolactone) blends exhibiting shape memory assisted self-healing (SMASH). ACS Appl Mater Interfaces 2011;3:152-161.
25. Averous L, Moro L, Dole P, Fringant C. Properties of thermoplastic blends: starch-polycaprolactone. Polymer 2000;41:4157-4167.
26. Li Z, Ramay HR, Hauch KD, Xiao D, Zhang M. Chitosan-alginate hybrid scaffolds for bone tissue engineering. Biomaterials 2005;26:3919-3928.
27. Wu F, Liu C, Neill B, Wei J, Ngothai Y. Fabrication and properties of porous scaffold of magnesium phosphate/polycaprolactone biocomposite for bone tissue engineering. Appl Surf Sci 2012;258:7589-7595.
28. Qiao C, Jiang S, Dong D, Ji X, An L, Jiang B. The critical lowest molecular weight for PEG to crystallize in cross-linked networks. Macromol Rapid Commun 2004;25:659-663.
29. Cai L, Lu J, Sheen V, Wang S. Lubricated biodegradable polymer networks for regulating nerve cell behavior and fabricating nerve conduits with a compositional gradient. Biomacromolecules 2012;13:358-368.
30. Chen DZ, Tang CY, Chan KC, Tsui CP, Yu PHF, Leung MCP, et al. Dynamic mechanical properties and in vitro bioactivity of PHBHV/HA nanocomposite. Compos Sci Technol 2007;67:1617-1626.

31. Koupaei N, Karkhaneh A, Daliri Joupari M. Preparation and characterization of (PCL-crosslinked-PEG)/hydroxyapatite as bone tissue engineering scaffolds. J Biomed Mater Res A 2015;103:919-3926.
32. Nazhat SN, Kellomäki M, Törmälä P, Tanner KE, Bonfield W. Dynamic mechanical characterization of biodegradable composites of hydroxyapatite and polylactides. J Biomed Mater Res 2001;58:335-343.
33. Shokrollahi P, Mirzadeh H, Scherman OA, Huck WT. Biological and mechanical properties of novel composites based on supramolecular polycaprolactone and functionalized hydroxyapatite. J Biomed Mater Res A 2010;95:209-221.
34. Misra SK, Ansari T, Mohn D, Valappil SP, Brunner TJ, Stark WJ, et al. Effect of nanoparticulate bioactive glass particles on bioactivity and cytocompatibility of poly(3-hydroxybutyrate) composites. J R Soc Interface 2010;7:453-465.
35. Fong P, Shinoka T, Lopez-Soler RI, Breuera C. The use of polymer based scaffolds in tissue-engineered heart valves. Prog Ped Cardio 2006;21:193-199.